

AER1216 - Fundamentals of UAS

Project Report

Aditya Jain (1007150351)
Apurv Mishra (1006695211)
Jigme Tsering (1007441975)



Institute for Aerospace Studies
University of Toronto
19th December, 2021

Contents

1	Overview	1
2	Fixed-Wing sUAS Development	2
2.1	Performance	2
2.2	Model Dynamics	3
2.3	Linearization	3
2.4	Altitude-Hold and Level-Coordinated Turn Controller	4
2.5	Simulation Results	5
3	Multi-Rotor Drone Development	7
3.1	Performance	7
3.2	Model Dynamics	8
3.3	Linearization	8
3.4	Position Controller	8
3.5	Simulation Results	9
4	Conclusions and Lessons Learned	11
A	Appendix	13
A.1	Aerosonde UAV Configuration	13
A.2	Equations of Motion State Variables	13
A.3	Inertia Parameters	14
A.4	State-space Coefficients for Fixed-Wing Linear Model	14
A.5	Linear State-space Models for Multi-rotor	15

List of Figures

1	Altitude-Hold and Coordinated-Turn for Fixed-wing	5
2	Simulation plots for steady-level	5
3	Simulation plots for coordinated-turn	6
4	Simulation plots for descend	6
5	Multi-rotor power requirement	7
6	Position/Orientation control for Multi-rotor	9
7	Simulation plots for each coordinate	10
8	3D Trajectory followed by the quadrotor	10

List of Tables

1	Parameters of Aerosonde UAV	13
2	State variables for equations of motion	13
3	Longitudinal state-space model coefficients	14
4	Lateral state-space model coefficients	15

1 Overview

This project covers the elaborate process of design and simulation of small Unmanned Aerial Systems (sUAS) for different scenarios, along with performance analysis and dynamics modelling. In this project, we worked on two configurations, one each for a fixed-wing and a multi-rotor. The given fixed-wing sUAS is the Aerosonde UAV and the multi-rotor is a quadrotor drone with custom configuration.

For each of the two aircraft systems, we perform the following tasks: 1) performance is evaluated in terms of flight range and endurance, 2) derivation of nonlinear dynamics model followed by linearization, 3) controller design in Simulink and 4) thorough simulation analysis of the controller for various tasks.

For the fixed-wing, an attitude-hold and speed control system is developed. This ensures that the aerial vehicle maintains the desired altitude and forward velocity. The aircraft is simulated to do a steady-level flight at an altitude of 2000 m, for a distance of 1000 m. Next, it does a 180 degree level-coordinated turn. It then descends to 1000 m followed by a steady-level flight. The corresponding values for trim conditions were calculated and used.

For the multi-rotor, we develop a position/orientation controller with state estimation integrated in a Simulink model. The quadrotor is given a sequence of positions in the three-dimensional space. The system, then, computes and performs the required motion to reach the desired positions. The complete system has three subsystems - position controller, dynamics model and position estimation.

This project showcases the fundamental working of an unmanned aerial system in fixed-wing and multi-rotor configurations. The growing applications of these systems and the increasing human dependency on them has been conspicuous in the last few years. The different use-cases demand different aircraft configurations. For example, a military drone that does surveillance is fundamentally different from a drone that does package delivery. Rigorous simulation analysis is required before such systems are built and tested in the real-world. Another important aspect is autonomy where stable controller design is an essential component. This project is focused on these two aspects and is a pre-cursor in any aircraft development process.

2 Fixed-Wing sUAS Development

The given fixed-wing system is an Aerosonde UAV [2] with a custom configuration outlined in table 1 and a 16×8 propeller .

2.1 Performance

The performance metrics of the specified aircraft is measured in terms of maximum range and maximum endurance. Range depends on the engine performance, based on fuel consumption rate, and is interpreted as the distance that an aircraft travels on one full tank. Since Aerosonde UAV is propeller-based, the first step is to calculate the specific fuel consumption (SFC), $c_p = \frac{-\dot{W}_f}{P}$.

The minimum power condition gives the maximum SFC and, thus, the maximum range. The following equations were used to calculate the velocity and minimum required power:

$$V_{P_{min}} = \sqrt{\frac{2W/S}{\rho(C_L)_{P_{min}}}} \quad (1)$$

$$P_{min} = \frac{W}{(C_L)_{P_{min}}} (4C_{D0}) V_{P_{min}} \quad (2)$$

Using power calculated in (2), the SFC is determined. Velocity from (1) and UIUC data for the given propeller [3] gives the efficiency. The corresponding maximum range is given by:

$$R_{max} = \frac{(\eta/c_p)}{2\sqrt{KC_{D0}}} (\ln \frac{W_0}{W_1}) \quad (3)$$

where W_0 = initial weight with a full tank and W_1 = aircraft weight without fuel, such that $W_0 - W_1 = W_f$ = fuel weight. Using data from the above equations, we calculate the below parameters for two altitudes:

At 1000 m: $V_{1000} = 14.82$ m/s, $P_{1000} = 119.48$ W, $c_{p1000} = 1.81e^{-06}$, $\eta_{1000} = 0.7831$

At 2000 m: $V_{2000} = 15.58$ m/s, $P_{2000} = 125.56$ W, $c_{p2000} = 1.73e^{-06}$, $\eta_{1000} = 0.7952$

Range values using (3): $(R_{max})_{1000} = 2,381.7$ km and $(R_{max})_{2000} = 2,541.6$ km

Next, we calculate the maximum endurance at the minimum thrust condition:

$$T_{R_{min}} = 2\sqrt{KC_{D0}}W \quad (4)$$

$$V_{T_{min}} = \sqrt{\frac{2W/S}{\rho(C_L)_{T_{min}}}} \quad (5)$$

The required power is calculated using thrust and velocity from (4) and (5). Like before, efficiency is calculated using velocity from (5) and UIUC data for the given propeller [3]. Thus, the maximum endurance is given by

$$E_{max} = \frac{\eta}{c_p} \sqrt{2\rho S_{prop}} \left(\frac{C_L^{3/2}}{C_D} \right)_{max} \left[\frac{1}{\sqrt{W_1}} - \frac{1}{\sqrt{W_0}} \right] \quad (6)$$

where $\left(\frac{C_L^{3/2}}{C_{D0}}\right)_{max} = \frac{1}{4C_{D0}} \left(\frac{3C_{D0}}{K}\right)^{3/4}$. Again, using the calculated data from above equations, we calculate different parameters for the two given altitudes.

At 1000 m: $V_{1000} = 19.51$ m/s, $P_{1000} = 136.18$ W, $c_{p1000} = 1.59e^{-06}$, $\eta_{1000} = 0.8278$
 At 2000 m: $V_{2000} = 20.50$ m/s, $P_{2000} = 143.11$ W, $c_{p2000} = 1.51e^{-06}$, $\eta_{1000} = 0.8291$

Endurance values using (6): $(E_{max})_{1000} = 20.96$ hours and $(E_{max})_{2000} = 23.18$ hours

2.2 Model Dynamics

The first step in controller design is to derive the non-linear dynamics model for a general fixed-wing aircraft. The twelve state variables used in the equations of motion are defined in table 2. The translational velocity components of the aircraft (u, v, w) are defined in the body-fixed frame, whereas, the translational position (p_n, p_e, p_d) is expressed in an inertial reference frame. Equation (7) is the kinematic relation between these two quantities. Equation (9) illustrates a similar expression for the body-frame angular rates (p, q, r) and the angular positions (ϕ, θ, ψ) . We then apply Newton's second law of motion to the translational and rotation degrees of freedom to derive the dynamics equations of motions (8) and (10), where inertial parameters Γ are defined in appendix A.3, $c_x = \cos x$, and $s_x = \sin x$. (f_x, f_y, f_z) and (l, m, n) are the externally applied forces and moments on the aircraft respectively.

$$\begin{pmatrix} \dot{p}_n \\ \dot{p}_e \\ \dot{p}_d \end{pmatrix} = \begin{pmatrix} c_\theta c_\psi & s_\phi s_\theta c_\psi - c_\phi s_\psi & c_\phi s_\theta c_\psi + s_\phi s_\psi \\ c_\theta s_\psi & s_\phi s_\theta s_\psi + c_\phi c_\psi & c_\phi s_\theta s_\psi - s_\phi c_\psi \\ -s_\theta & s_\phi c_\theta & c_\phi c_\theta \end{pmatrix} \begin{pmatrix} u \\ v \\ w \end{pmatrix} \quad (7)$$

$$\begin{pmatrix} \dot{u} \\ \dot{v} \\ \dot{w} \end{pmatrix} = \begin{pmatrix} rv - qw \\ pw - rv \\ qu - pv \end{pmatrix} + \frac{1}{m} \begin{pmatrix} f_x \\ f_y \\ f_z \end{pmatrix} \quad (8)$$

$$\begin{pmatrix} \dot{\phi} \\ \dot{\theta} \\ \dot{\psi} \end{pmatrix} = \begin{pmatrix} 1 & \sin\phi \tan\theta & \cos\phi \tan\theta \\ 0 & \cos\phi & -\sin\phi \\ 0 & \frac{\sin\phi}{\cos\theta} & \frac{\cos\phi}{\sin\theta} \end{pmatrix} \begin{pmatrix} p \\ q \\ r \end{pmatrix} \quad (9)$$

$$\begin{pmatrix} \dot{p} \\ \dot{q} \\ \dot{r} \end{pmatrix} = \begin{pmatrix} \Gamma_1 pq - \Gamma_2 qr \\ \Gamma_5 pr - \Gamma_6 (p^2 - r^2) \\ \Gamma_7 pq - \Gamma_1 qr \end{pmatrix} + \begin{pmatrix} \Gamma_3 l + \Gamma_4 n \\ \frac{1}{I_{yy}} m \\ \Gamma_4 l + \Gamma_8 n \end{pmatrix} \quad (10)$$

2.3 Linearization

The dynamics equations presented in the preceding section are non-linear and coupled in nature. It's hard to design controllers for such systems. In this section, we decouple the dynamics equations into longitudinal and lateral motions of the aircraft and linearize them. Following the procedure in chapter 5 of [1], (11) and (12) are the final linearized state-space equations for longitudinal and lateral motions respectively.

$$\begin{pmatrix} \dot{\bar{u}} \\ \dot{\bar{w}} \\ \dot{\bar{q}} \\ \dot{\bar{\theta}} \\ \dot{\bar{h}} \end{pmatrix} = \begin{pmatrix} X_u & X_w & X_q & -g\cos\theta^* & 0 \\ Z_u & Z_w & Z_q & -g\sin\theta^* & 0 \\ M_u & M_w & M_q & 0 & 0 \\ 0 & 0 & 1 & 0 & 0 \\ \sin\theta^* & -\cos\theta^* & 0 & u^*\cos\theta^* + w^*\sin\theta^* & 0 \end{pmatrix} \begin{pmatrix} \bar{u} \\ \bar{w} \\ \bar{q} \\ \bar{\theta} \\ \bar{h} \end{pmatrix} + \begin{pmatrix} X_{\delta_e} & X_{\delta_t} \\ Z_{\delta_e} & 0 \\ M_{\delta_e} & 0 \\ 0 & 0 \\ 0 & 0 \end{pmatrix} \begin{pmatrix} \bar{\delta}_e \\ \bar{\delta}_t \end{pmatrix} \quad (11)$$

$$\begin{pmatrix} \dot{\bar{v}} \\ \dot{\bar{p}} \\ \dot{\bar{r}} \\ \dot{\bar{\phi}} \\ \dot{\bar{\psi}} \end{pmatrix} = \begin{pmatrix} Y_v & Y_p & Y_r & g\cos\theta^*\cos\phi^* & 0 \\ L_v & L_p & L_r & 0 & 0 \\ N_v & N_p & N_r & 0 & 0 \\ 0 & 1 & \cos\phi^*\tan\phi^* & q^*\cos\phi^*\tan\theta^* - r^*\sin\phi^*\tan\theta^* & 0 \\ 0 & 0 & \cos\phi^*\sec\theta^* & p^*\cos\phi^*\sec\theta^* - r^*\sin\phi^*\sec\theta^* & 0 \end{pmatrix} \begin{pmatrix} \bar{v} \\ \bar{p} \\ \bar{r} \\ \bar{\phi} \\ \bar{\psi} \end{pmatrix} + \begin{pmatrix} Y_{\delta_a} & Y_{\delta_r} \\ L_{\delta_a} & L_{\delta_r} \\ N_{\delta_a} & N_{\delta_r} \\ 0 & 0 \\ 0 & 0 \end{pmatrix} \begin{pmatrix} \bar{\delta}_a \\ \bar{\delta}_r \end{pmatrix} \quad (12)$$

The linearization is done around an equilibrium condition called *trim*, where the forces and moments on the aircraft are balanced. The trim states (variables with *) in equations (11), (12) are calculated for constant-altitude, wings-level steady flight. This condition sets the variables γ^* , v^* , ϕ^* , ψ^* , p^* , q^* , r^* , β^* , δ_a^* , δ_r^* to zero. Balancing lift and weight gives:

$$\alpha^* = \frac{mg - \frac{1}{2}\rho V_a^2 SC_{L0}}{C_{L\alpha} \times \frac{1}{2}\rho V_a^2 S} = 0.2671$$

Thus, $\theta^* = \gamma^* + \alpha^* = 0.2671$. Similarly δ_t^* ($=0.8311$) is obtained by balancing thrust and drag. Elevator deflection angle is estimated from $M=0$, which leads to the following expression:

$$\delta_e^* = \frac{-C_{m0} - C_{m\alpha}\alpha^*}{C_{m\delta_e}} = -0.15616$$

Using the wind triangle, $u^* = 18.33m/s$ and $w^* = 5.01m/s$.

2.4 Altitude-Hold and Level-Coordinated Turn Controller

The altitude-hold controller is designed to keep the flight at constant speed and altitude. The desired altitude and forward speed are given as inputs to elevator and throttle/propeller controls, respectively. The difference between the current and desired values are fed into the individual tuned PID blocks for minimizing the error.

The level-coordinated turn controller turns the aircraft with a desired radius and angle, while maintaining its altitude and having zero lateral acceleration. The required turn rate and side-slip velocity are given as inputs to the control of rudder and aileron, respectively. For a velocity V and radius of curvature R , the required turn rate $\dot{\psi} = \frac{V}{R}$ and the corresponding bank angle $\phi = \frac{V\dot{\psi}}{g}$. For $V = 19m/s$ and $R = 250m$, $\dot{\psi} = 0.076s^{-1}$. The combined Simulink controller design for the two tasks is shown in figure 1.

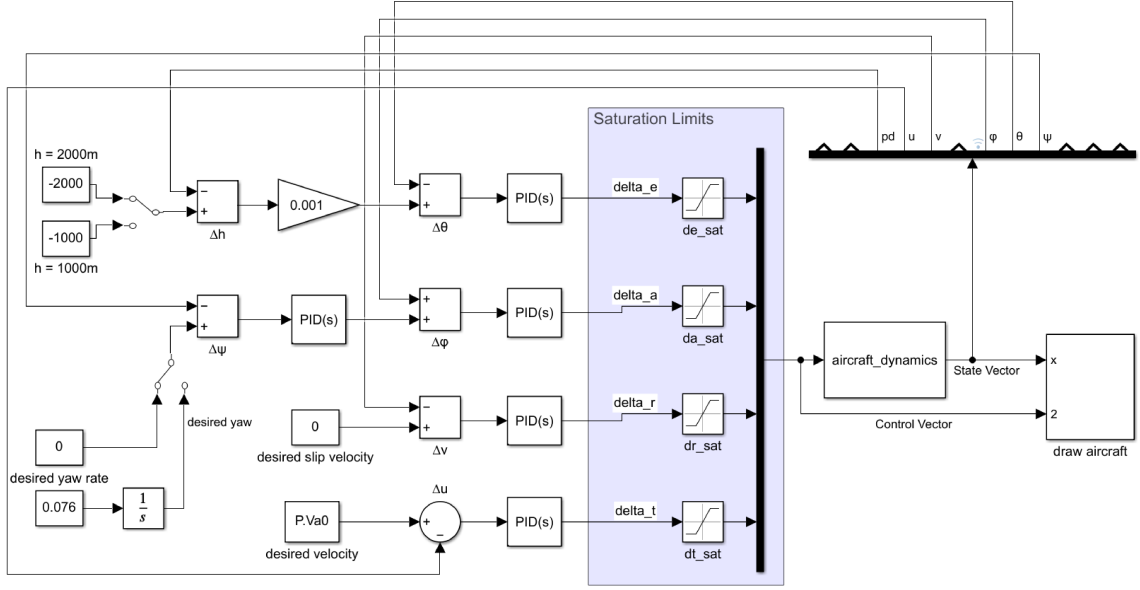


Figure 1: Altitude-Hold and Coordinated-Turn for Fixed-wing

2.5 Simulation Results

First, the controller was given a desired altitude of 2000 m and the desired velocity as 19 m/s. The simulation plots in figure 2 depict that a steady-level flight is maintained with an error of +5 m in altitude and 0.2 m/s in forward speed, that later gets stabilized.

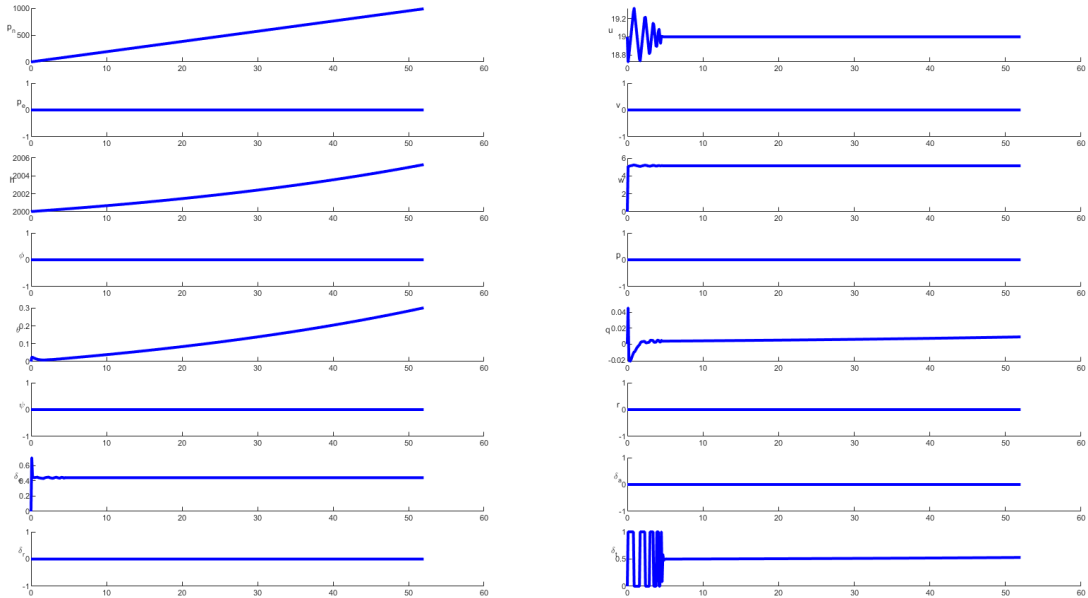


Figure 2: Simulation plots for steady-level

Next, for the level-coordinated turn, the desired yaw rate (calculated in section 2.4) and the desired side-slip velocity ($=0$) are given as inputs. The plots in figure 3 show that a turn of 180 degrees is completed at a radius of curvature of 250 m, altitude is held at roughly 2000 m and a net displacement of 0 m in p_n and 500 m in p_e .

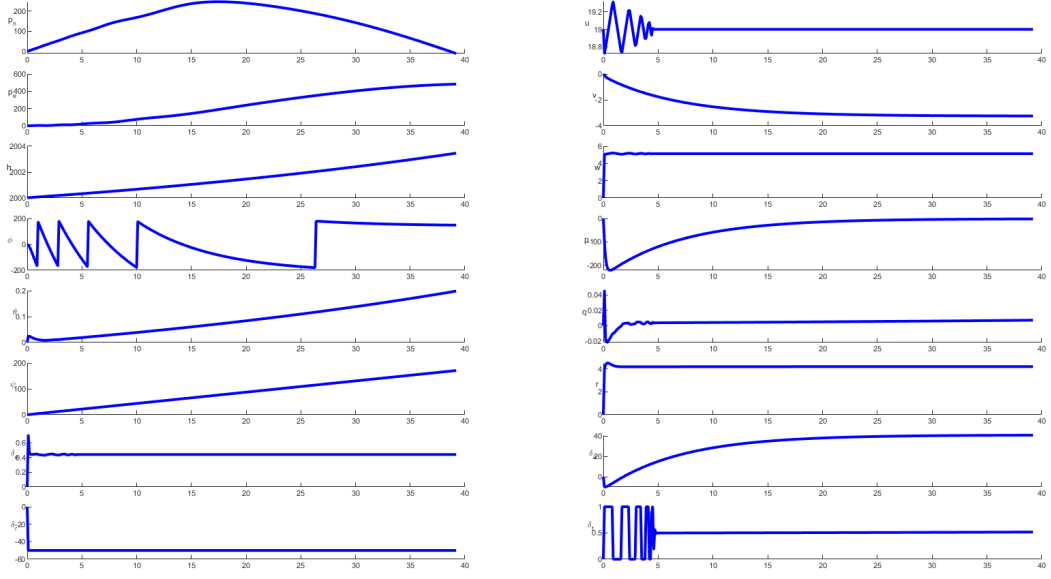


Figure 3: Simulation plots for coordinated-turn

Lastly, a descend of 100 m is performed from 2000 m by changing the desired altitude input. The results are shown in figure 4.

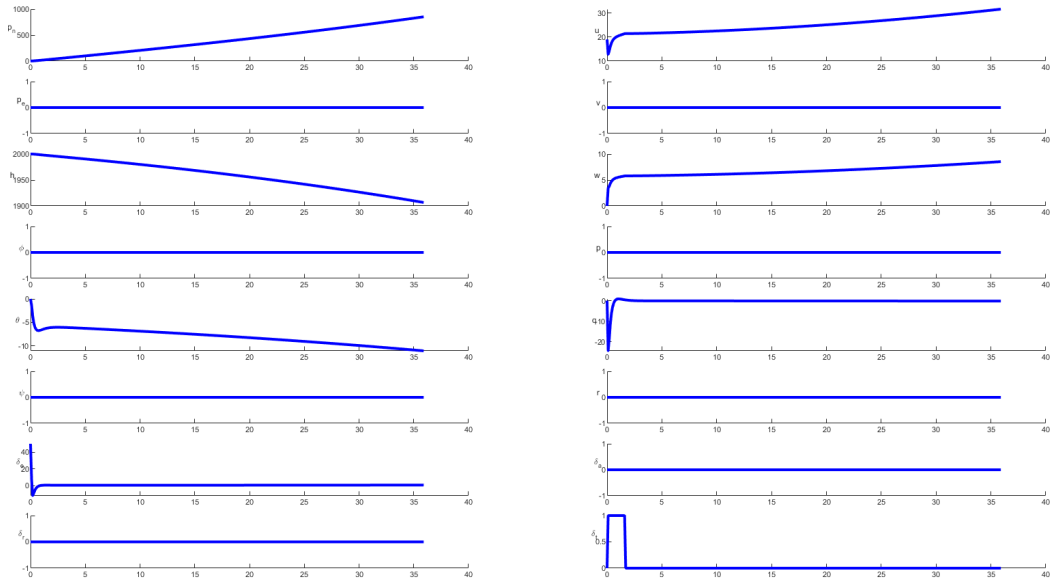


Figure 4: Simulation plots for descend

3 Multi-Rotor Drone Development

The multi-rotor drone is a quadrotor with a total weight of 420 gm, $C_D = 0.97$, and a reference area $S = 0.01 \text{ m}^2$. It uses four APC 8x6 Slow Flyer propellers and powered by a 3 cell 1500 mAh battery.

3.1 Performance

The performance of the quadrotor configuration is calculated in terms of range and endurance for a forward flight. The first step is to calculate the total energy in the battery $E_b = (\text{No. Cells}) \times 3.7 \times \text{mA-hr}/1000 \times 3600 = 59940 \text{ J}$. Next, total power required by the quadrotor is calculated for forward velocities V ranging from 0 to 40 m/sec using equation (13) derived from forward flight-momentum theory.

$$P_{total} = T(v + V \sin \alpha_D) \quad (13)$$

where $\alpha_D = \tan^{-1}(D/W)$, $D = 1/2 \rho S C_D V^2$ and v is the induced velocity calculated using (14).

$$v^4 + (2V \sin \alpha_D)v^3 + V^2v^2 - (W^2 + D^2)/(2\rho A)^2 = 0 \quad (14)$$

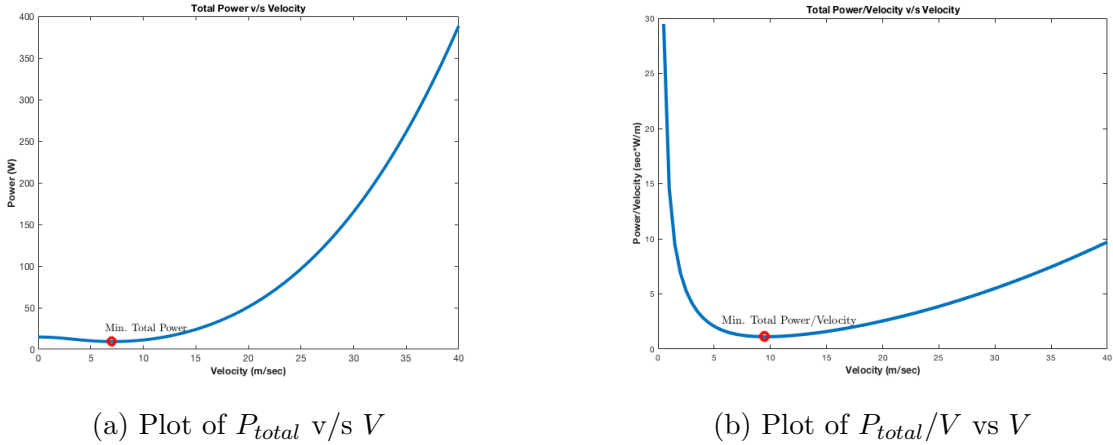


Figure 5: Multi-rotor power requirement

Figure 5a plots the total power required by the drone as a function of forward velocity. The quadrotor should fly with the velocity V (7 m/sec) corresponding to the minimum P_{total} (9.3 W) for maximum endurance. Using equation (15), the endurance was found to be 68.2 min.

$$t_e = E_b \eta_m \eta_e / P_{total} \quad (15)$$

where $\eta_m = 75\%$ is the motor efficiency and $\eta_e = 85\%$ is the ESC efficiency.

The quadrotor will have maximum range for the forward velocity V corresponding to the minimum P_{total}/V . Figure 5b illustrates this with the minimum occurring at $V = 9.5$ m/sec and $P_{total} = 10.6 \text{ W}$. For this P_{total} and using equation (15), the flying time for maximum range $t_R = 59.8 \text{ min}$. Finally, the maximum range $R_{max} = t_R \times V = 34 \text{ km}$.

3.2 Model Dynamics

Similar to the fixed-wing, the multi-rotor configuration has twelve state variables defined in different reference frames, that are enumerated in table 2. Equations (16) and (18) define the kinematics, while the system dynamics are represented by equations (17) and (19) using Newton's laws of motion and equation of Coriolis. The variables are defined as follows: τ = torque, m = total mass of vehicle, F = total thrust from rotors, g = acceleration due to gravity, $I_{()}$ = moment of inertia, $c_x = \cos x$ and $s_x = \sin x$.

$$\begin{pmatrix} \dot{p}_n \\ \dot{p}_e \\ \dot{p}_d \end{pmatrix} = \begin{pmatrix} c_\theta c_\psi & s_\phi s_\theta c_\psi - c_\phi s_\psi & c_\phi s_\theta c_\psi + s_\phi s_\psi \\ c_\theta s_\psi & s_\phi s_\theta s_\psi + c_\phi c_\psi & c_\phi s_\theta s_\psi - s_\phi c_\psi \\ -s_\theta & s_\phi c_\theta & c_\phi c_\theta \end{pmatrix} \begin{pmatrix} u \\ v \\ w \end{pmatrix} \quad (16)$$

$$\begin{pmatrix} \dot{u} \\ \dot{v} \\ \dot{w} \end{pmatrix} = \begin{pmatrix} rv - qw \\ pw - rv \\ qu - pv \end{pmatrix} + \begin{pmatrix} -g \sin \theta \\ g \cos \theta \sin \phi \\ g \cos \theta \cos \phi \end{pmatrix} + \frac{1}{m} \begin{pmatrix} 0 \\ 0 \\ -F \end{pmatrix} \quad (17)$$

$$\begin{pmatrix} \dot{\phi} \\ \dot{\theta} \\ \dot{\psi} \end{pmatrix} = \begin{pmatrix} 1 & \sin \phi \tan \theta & \cos \phi \tan \theta \\ 0 & \cos \phi & -\sin \phi \\ 0 & \frac{\sin \phi}{\cos \theta} & \frac{\cos \phi}{\sin \theta} \end{pmatrix} \begin{pmatrix} p \\ q \\ r \end{pmatrix} \quad (18)$$

$$\begin{pmatrix} \dot{p} \\ \dot{q} \\ \dot{r} \end{pmatrix} = \begin{pmatrix} \frac{I_{yy} - I_{zz}}{I_{xx}} qr \\ \frac{I_{zz} - I_{xx}}{I_{yy}} pr \\ \frac{I_{xx} - I_{yy}}{I_{zz}} pq \end{pmatrix} + \begin{pmatrix} \frac{1}{I_{xx}} \tau_\phi \\ \frac{1}{I_{yy}} \tau_\theta \\ \frac{1}{I_{zz}} \tau_\psi \end{pmatrix} \quad (19)$$

3.3 Linearization

A linearized dynamics model is derived when the multi-rotor is at an equilibrium position. Taylor series expansion is used for approximation, that eases the process of controller design. The process first involves calculation of the equilibrium points by equating the net force and moment to zero. Then the state variable derivatives are approximated using Taylor series expansion, where the Jacobians are calculated at equilibrium points.

The provided linear state-space model, as given in Appendix A.5, accepts a desired value and provides a current value. The inputs and outputs for the state-space models are described in the next section.

3.4 Position Controller

A position/orientation controller takes the desired position as input and calculates the parameters for the multi-rotor to reach the desired position. The desired Euler angles and rates correspond to the difference between the desired and current position values. This difference defines the error in position which is later minimized.

The *position controller* block in figure 6 calculates the error in position and subtracts it from corresponding Euler parameter. The net error is then using PID controller. For vertical dynamics, the input is the desired vertical velocity.

The *dynamic model* block is the implementation of the given state-space model. It takes the inputs from the tuned PID blocks and provides current values as per the following state-flow:

desired roll angle $\xrightarrow{\text{roll dynamics}}$ current roll angle $\xrightarrow{\text{roll to } v}$ current side velocity
 desired pitch angle $\xrightarrow{\text{pitch dynamics}}$ current pitch angle $\xrightarrow{\text{pitch to } u}$ current forward velocity
 desired yaw rate $\xrightarrow{\text{yaw dynamics}}$ current yaw angle
 desired vertical velocity $\xrightarrow{\text{vertical dynamics}}$ current height

The *position estimation* block takes as input the Euler angles and calculates the body-to-earth rotation matrix. This matrix is used to transform the body-frame velocities to inertial-frame velocities. These transformed velocities are then integrated to give current position in inertial reference frame.

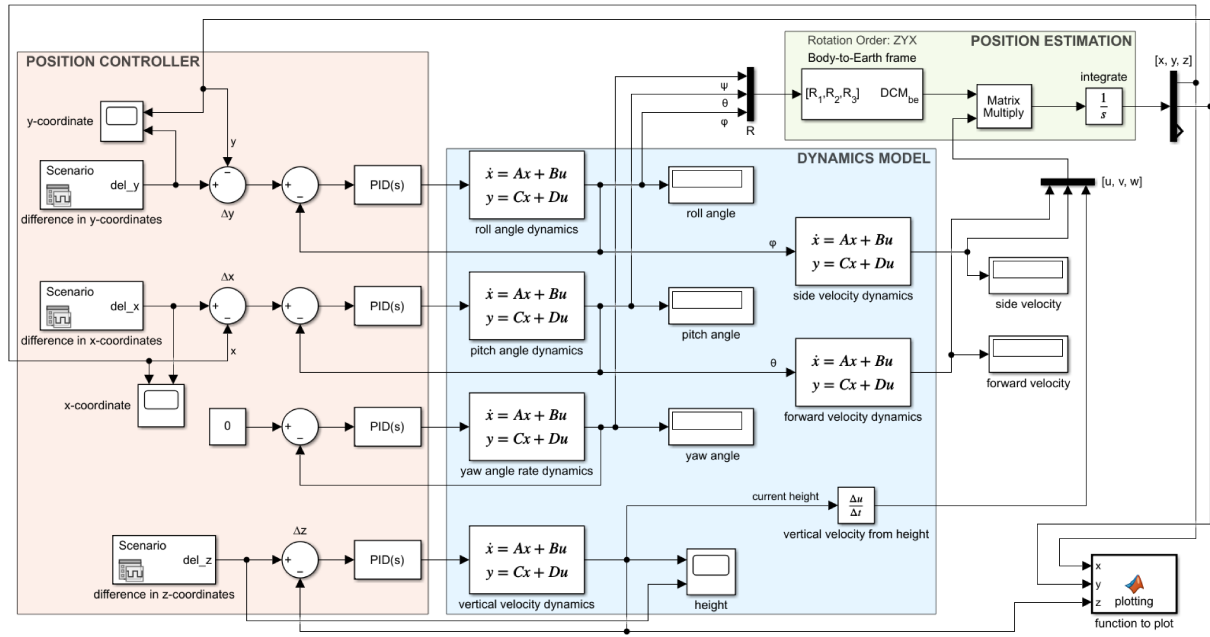


Figure 6: Position/Orientation control for Multi-rotor

3.5 Simulation Results

To test the controller, the quadrotor is made to fly through a sequence of positions in three-dimensional space. The vehicle hovers for 10 seconds before flying to the next coordinate. The sequence of coordinates are $\{0, 0, 2\}$, $\{5, 6, 4\}$, $\{-5, -6, 4\}$ and back to $\{0, 0, 2\}$. Figure 7 shows the motion of the aircraft for each axes separately and figure 8 is a three-dimensional plot for the same aircraft trajectory.

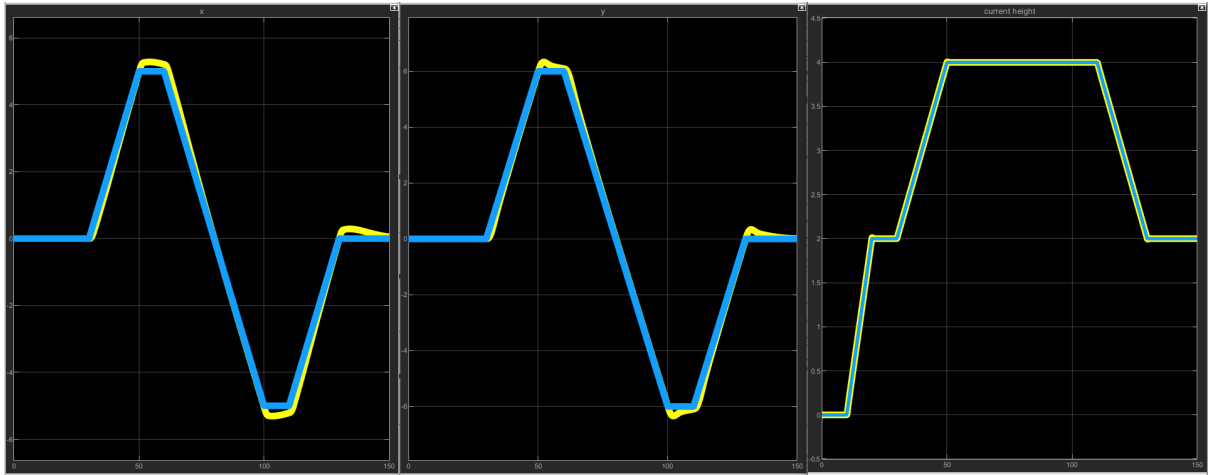


Figure 7: Simulation plots for each coordinate

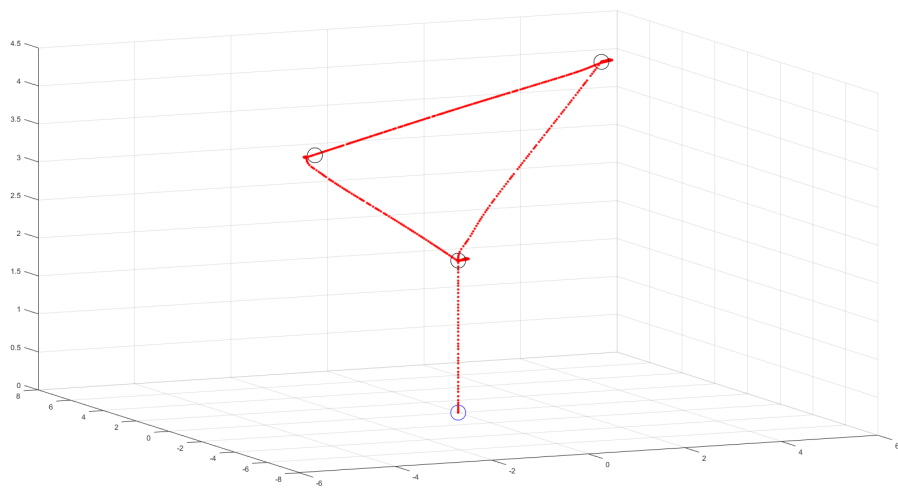


Figure 8: 3D Trajectory followed by the quadrotor

4 Conclusions and Lessons Learned

The primary focus of this project is to develop control designs for an autonomous flight of an unmanned aerial system. Our work envelops the performance analysis of the given aircraft configurations, derivation of the non-linear dynamics model followed by linearization and lastly, development and simulation analysis of controllers in Simulink.

We notice that the flight stability depends significantly on the correctness of the trim calculations. Multiple revisions of the trim values lead to an increased stability. For the level-coordinated turn, the required yaw rate is calculated from the desired turn radius and angle of rotation. The banking angle is another important parameter for a stable turn. The trim calculations change for the descend motion and the elevator deflection is non-zero, unlike the altitude-hold flight.

For fixed-wing performance, the maximum range is calculated at minimum power condition and the maximum endurance calculation is done at minimum thrust. In multi-rotor, the maximum endurance calculation is done at minimum power requirement while the maximum range is calculated for minimum power/velocity.

Throughout the project, some key lessons were learnt:

- It's important to interpret the physical significance of simulation results, especially understanding the unrealistic scenarios
- The system is quite sensitive to the correctness of trim and equilibrium values
- Non-linearized models are mathematically simpler to understand and derive but controller design is hard
- Linear dynamics models are comparatively tedious and complex to derive but designing, implementation and debugging of the controller becomes easier
- It is crucial to have good visualization tools to interpret the simulation results at various intermediate stages

The team worked on the project collaboratively with the following primary contributions 1) Aditya - dynamics modelling of fixed-wing, implementation of the fixed-wing linear model and performance analysis of multi-rotor, 2) Apurv - performance analysis of fixed-wing and dynamic modelling of multi-rotor with controller design and 3) Jigme - linearization of fixed-wing dynamics and trim calculations for different scenarios. Simulink models, presentation and project report had equal contribution from all team members.

References

- [1] Randal W Beard and Timothy W McLain. *Small unmanned aircraft*. Princeton university press, 2012.
- [2] Textron Systems. Aerosonde UAV. <https://www.textronsystems.com/products/aerosonde>.
- [3] Dept. of Aerospace Engineering UIUC. UIUC Propeller Database. <https://m-selig.ae.illinois.edu/props/volume-3/propDB-volume-3.html>.

A Appendix

A.1 Aerosonde UAV Configuration

Geometric		Longitudinal		Lateral	
Parameter	Value	Coef.	Value	Coef.	Value
m	13.5 kg	C_{L0}	0.28	C_{Y0}	0
I_{xx}	0.8244 kg m ²	C_{D0}	0.03	C_{l0}	0
I_{yy}	1.135 kg m ²	C_{m0}	-0.02338	C_{n0}	0
I_{zz}	1.759 kg m ²	$C_{L\alpha}$	3.45	$C_{Y\beta}$	-0.98
I_{xz}	0.1204 kg m ²	$C_{D\alpha}$	0.30	$C_{l\beta}$	-0.12
S	0.55 m ²	$C_{m\alpha}$	-0.38	$C_{n\beta}$	0.25
b	2.8956 m	C_{Lq}	0	C_{Yp}	0
c	0.18994 m	C_{Dq}	0	C_{lp}	-0.26
S_{prop}	0.1297 m ²	C_{mq}	-3.6	C_{Yp}	0
e	0.9	$C_{L\delta_e}$	-0.36	C_{Yr}	0
Ω_{max}	7000 RPM	$C_{D\delta_e}$	0	C_{lr}	0.14
Fuel Capacity	5.7 L	$C_{m\delta_e}$	-0.5	C_{nr}	-0.35
		ϵ	0.1592	$C_{l\delta_a}$	0.08
				$C_{n\delta_a}$	0.06
				$C_{Y\delta_r}$	-0.17
				$C_{l\delta_r}$	0.105
				$C_{n\delta_r}$	-0.032

Table 1: Parameters of Aerosonde UAV

A.2 Equations of Motion State Variables

Name	Description
p_n	Inertial north position
p_e	Inertial east position
p_d	Inertial down position
u	Body frame velocity along i^b
v	Body frame velocity along j^b
w	Body frame velocity along k^b
ϕ	Roll angle
θ	Pitch angle
ψ	Yaw angle
p	Roll rate along i^b
q	Pitch rate along j^b
r	Yaw rate along k^b

Table 2: State variables for equations of motion

A.3 Inertia Parameters

The fixed-wing inertia parameters used in the non-linear dynamics equations:

$$\begin{aligned}
\Gamma &= I_{xx}I_{zz} - I_{xz}^2 \\
\Gamma_1 &= \frac{I_{xz}(I_{xx} - I_{yy} + I_{zz})}{\Gamma} \\
\Gamma_2 &= \frac{I_{zz}(I_{zz} - I_{yy}) + I_{xz}^2}{\Gamma} \\
\Gamma_3 &= \frac{I_{zz}}{\Gamma} \\
\Gamma_4 &= \frac{I_{xz}}{\Gamma} \\
\Gamma_5 &= \frac{I_{zz} - I_{xx}}{\Gamma} \\
\Gamma_6 &= \frac{I_{xz}}{\Gamma} \\
\Gamma_7 &= \frac{(I_{xx} - I_{yy})I_{xx} + I_{xz}^2}{\Gamma} \\
\Gamma_8 &= \frac{I_{xx}}{\Gamma}
\end{aligned}$$

A.4 State-space Coefficients for Fixed-Wing Linear Model

Longitudinal	Formula
X_u	$\frac{u^*\rho S}{m}[C_{X_0} + C_{X_\alpha}\alpha^* + C_{X_{\delta_e}}\delta_e^*] - \frac{\rho S w^* C_{X_\alpha}}{2m} + \frac{\rho S c C_{X_q} u^* q^*}{4m V_a^*} - \frac{\rho S_{prop} C_{prop} u^*}{m}$
X_w	$-q^* + \frac{w^*\rho S}{m}[C_{X_0} + C_{X_\alpha}\alpha^* + C_{X_{\delta_e}}\delta_e^*] + \frac{\rho S c C_{X_q} w^* q^*}{4m V_a^*} + \frac{\rho S c C_{X_\alpha} u^*}{4m V_a^*} - \frac{\rho S_{prop} C_{prop} w^*}{m}$
X_q	$-w^* + \frac{\rho V_a^* S C_{X_q} c}{4m}$
X_{δ_e}	$\frac{\rho V_a^* S C_{X_{\delta_e}}}{4m}$
X_{δ_t}	$\frac{\rho S_{prop} C_{prop} k^2 \delta_t^*}{m}$
Z_u	$q^* + \frac{u^*\rho S}{m}[C_{Z_0} + C_{Z_\alpha}\alpha^* + C_{Z_{\delta_e}}\delta_e^*] - \frac{\rho S C_{Z_\alpha} w^*}{2m} + \frac{u^*\rho S c C_{Z_q} c q^*}{4m V_a^*}$
Z_w	$\frac{w^*\rho S}{m}[C_{Z_0} + C_{Z_\alpha}\alpha^* + C_{Z_{\delta_e}}\delta_e^*] - \frac{\rho S C_{Z_\alpha} u^*}{2m} + \frac{\rho S c C_{Z_q} c q^*}{4m V_a^*}$
Z_q	$u^* + \frac{\rho V_a^* S C_{Z_q} c}{4m}$
Z_{δ_e}	$\frac{\rho V_a^* S C_{Z_{\delta_e}}}{4m}$
M_u	$\frac{u^*\rho S c}{I_{yy}}[C_{m_0} + C_{m_\alpha}\alpha^* + C_{m_{\delta_e}}\delta_e^*] - \frac{\rho S c C_{m_\alpha} w^*}{2I_{yy}} + \frac{\rho S c^2 C_{m_q} u^* q^*}{4I_{yy} V_a^*}$
M_w	$\frac{w^*\rho S c}{m}[C_{m_0} + C_{m_\alpha}\alpha^* + C_{m_{\delta_e}}\delta_e^*] + \frac{\rho S c C_{m_\alpha} u^*}{2I_{yy}} + \frac{\rho S c^2 C_{m_q} u^* q^* w^*}{4I_{yy} V_a^*}$
M_q	$\frac{\rho V_a^* S c^2 C_{m_q}}{4I_{yy}}$
M_{δ_e}	$\frac{\rho V_a^* S c C_{m_{\delta_e}}}{2I_{yy}}$

Table 3: Longitudinal state-space model coefficients

<i>Lateral</i>	<i>Formula</i>
Y_v	$\frac{\rho S b v^*}{4m V_a^*} [C_{Y_p} p^* + C_{Y_r} r^*] + \frac{\rho S v^*}{m} [C_{Y_0} + C_{Y_\beta} \beta^* + C_{Y_{\delta a}} \delta_a^* + C_{Y_{\delta r}} \delta_r^*] + \frac{\rho S C_{Y_\beta}}{2m} \sqrt{u^{*2} + w^{*2}}$
Y_p	$w^* + \frac{\rho V_a^* S b}{4m} C_{Y_p}$
Y_r	$-u^* + \frac{\rho V_a^* S b}{4m} C_{Y_r}$
$Y_{\delta a}$	$\frac{\rho V_a^* S}{2m} C_{Y_{\delta a}}$
$Y_{\delta r}$	$\frac{\rho V_a^* S}{2m} C_{Y_{\delta r}}$
L_v	$\frac{\rho S b^2 v^*}{4V_a^*} [C_{p_p} p^* + C_{p_r} r^*] + \rho S b v^* [C_{p_0} + C_{p_\beta} \beta^* + C_{p_{\delta a}} \delta_a^* + C_{p_{\delta r}} \delta_r^*] + \frac{\rho S b C_{Y_\beta}}{2} \sqrt{u^{*2} + w^{*2}}$
L_p	$\Gamma_1 q^* + \frac{\rho V_a^* S b^2}{4} C_{p_p}$
L_r	$-\Gamma_2 q^* + \frac{\rho V_a^* S b^2}{4} C_{p_r}$
$L_{\delta a}$	$\frac{\rho V_a^* S b}{2} C_{p_{\delta a}}$
$L_{\delta r}$	$\frac{\rho V_a^* S b}{2} C_{p_{\delta r}}$
N_v	$\frac{\rho S b^2 v^*}{4V_a^*} [C_{r_p} p^* + C_{r_r} r^*] + \rho S b v^* [C_{r_0} + C_{r_\beta} \beta^* + C_{r_{\delta a}} \delta_a^* + C_{r_{\delta r}} \delta_r^*] + \frac{\rho S b C_{r_\beta}}{2} \sqrt{u^{*2} + w^{*2}}$
N_p	$\Gamma_7 q^* + \frac{\rho V_a^* S b^2}{4} C_{r_p}$
N_r	$-\Gamma_2 q^* + \frac{\rho V_a^* S b^2}{4} C_{r_r}$
$N_{\delta a}$	$\frac{\rho V_a^* S b}{2} C_{r_{\delta a}}$
$L_{\delta r}$	$\frac{\rho V_a^* S b}{2} C_{r_{\delta r}}$

Table 4: Lateral state-space model coefficients

A.5 Linear State-space Models for Multi-rotor

- Roll

$$A = \begin{bmatrix} -4.2683 & -3.1716 \\ 4 & 0 \end{bmatrix}, B = \begin{bmatrix} 2 \\ 0 \end{bmatrix}, C = [0.7417 \quad 0.4405] \text{ and } D = [0]$$

- Pitch

$$A = \begin{bmatrix} -3.9784 & -2.9796 \\ 4 & 0 \end{bmatrix}, B = \begin{bmatrix} 2 \\ 0 \end{bmatrix}, C = [1.2569 \quad 0.6083] \text{ and } D = [0]$$

- Yaw

$$A = [-0.0059], B = [1], C = [1.2653] \text{ and } D = [0]$$

- Height

$$A = \begin{bmatrix} -5.8200 & -3.6046e-6 \\ 3.8147e-6 & 0 \end{bmatrix}, B = \begin{bmatrix} 1024 \\ 0 \end{bmatrix}, C = [1.4907e-4 \quad 1.3191e3] \\ \text{and } D = [0]$$

- Pitch to u

$$A = [-0.665], B = \begin{bmatrix} 2 \\ 0 \end{bmatrix}, C = [-3.0772] \text{ and } D = [0]$$

- Roll to v

$$A = [-0.4596], B = \begin{bmatrix} 2 \\ 0 \end{bmatrix}, C = [2.3868] \text{ and } D = [0]$$